THE JOURNAL OF BIOLOGICAL CHEMISTRY
Vol. 279, No. 22, Issue of May 28, pp. 23364–23375, 2004

Printed in U.S.A.

A Gelsolin-like Protein from *Papaver rhoeas* Pollen (PrABP80) Stimulates Calcium-regulated Severing and Depolymerization of Actin Filaments*[S]

Received for publication, November 30, 2003, and in revised form, March 12, 2004
Published, JBC Papers in Press, March 22, 2004, DOI 10.1074/jbc.M312973200

Shanjin Huang‡, Laurent Blanchoin§¶, Faisal Chaudhry‡, Vernonica E. Franklin-Tong‖, and Christopher J. Staiger‡**

From the ‡Department of Biological Sciences and The Purdue Motility Group, Purdue University, West Lafayette, Indiana 47907-2064, the §Laboratoire de Physiologie Cellulaire Végétale, Commissariat à l'Energie Atomique (CEA)/CNRS/Université Joseph Fourier, CEA F38054 Grenoble, France, and the ‖School of Biosciences, University of Birmingham, Edgbaston, Birmingham B15 2TT, United Kingdom

The cytoskeleton is a key regulator of plant morphogenesis, sexual reproduction, and cellular responses to extracellular stimuli. During the self-incompatibility response of *Papaver rhoeas* L. (field poppy) pollen, the actin filament network is rapidly depolymerized by a flood of cytosolic free Ca^{2+} that results in cessation of tip growth and prevention of fertilization. Attempts to model this dramatic cytoskeletal response with known pollen actin-binding proteins (ABPs) revealed that the major G-actin-binding protein profilin can account for only a small percentage of the measured depolymerization. We have identified an 80-kDa, Ca^{2+}-regulated ABP from poppy pollen (PrABP80) and characterized its biochemical properties *in vitro*. Sequence determination by mass spectrometry revealed that PrABP80 is related to gelsolin and villin. The molecular weight, lack of filament cross-linking activity, and a potent severing activity are all consistent with PrABP80 being a plant gelsolin. Kinetic analysis of actin assembly/disassembly reactions revealed that substoichiometric amounts of PrABP80 can nucleate actin polymerization from monomers, block the assembly of profilin-actin complex onto actin filament ends, and enhance profilin-mediated actin depolymerization. Fluorescence microscopy of individual actin filaments provided compelling, direct evidence for filament severing and confirmed the actin nucleation and barbed end capping properties. This is the first direct evidence for a plant gelsolin and the first example of efficient severing by a plant ABP. We propose that PrABP80 functions at the center of the self-incompatibility response by creating new filament pointed ends for disassembly and by blocking barbed ends from profilin-actin assembly.

The plant cytoskeleton comprises a dynamic network of actin filaments, microtubules, and accessory proteins that powers cytoplasmic streaming, prevents fungal attack, patterns the deposition of cellulosic wall polymers, and shapes cellular morphogenesis. Understanding how the cytoskeleton is organized, how it responds to environmental cues, and how its dynamics are regulated are central questions in plant biology. In addition to being essential for sexual reproduction, pollen is an ideal choice of material for studies of the cytoskeleton. Actin is one of the most abundant proteins in pollen, representing 5–20% of total cellular protein (1, 2). Cytoskeletal genes are among the most abundantly expressed classes of transcripts in *Arabidopsis* pollen (3), and several classes of actin-binding protein (ABP)[1] have been isolated and characterized biochemically (4–6). Pollen tube growth is arguably the most dramatic example of cellular morphogenesis in plants (5, 7). A cytoplasmic extension of the vegetative cell, the pollen tube, carries the male gametes through the pistil at growth rates up to 1 cm/h. The tip growth mechanism involves carefully orchestrated delivery of cell wall materials and plasma membrane through the directed trafficking of secretory vesicles. Underlying this cellular expansion is a polar distribution of cytoplasmic organelles, oscillatory gradients of cytosolic ions, and a specific organization of the cytoskeletal machinery. Prominent actin cables support reverse fountain cytoplasmic streaming and are arranged axially throughout much of the cytoplasm. A collar-like zone of fine filament bundles, in the apical 10–15 μm, and a dynamic meshwork of fine actin filaments (F-actin) at the extreme apex are thought to organize vesicle docking and fusion. Although actin filament turnover is essential for pollen tube growth (8, 9), exactly how the cytoskeleton functions and what accessory factors modulate these events remain poorly understood.

Many plant species utilize genetic mechanisms to prevent inbreeding. The self-incompatibility (SI) response in field poppy (*Papaver rhoeas*) pollen involves a flood of cytosolic free calcium ($[Ca^{2+}]_i$) that correlates with the cessation of tip growth (10–12). Cytological and biochemical studies demonstrate that reorganization of the actin cytoskeleton is one of the earliest events triggered by SI (13, 14). Quantitative analyses of F-actin levels reveal a rapid and sustained depolymerization

* This work was supported by grants from the Department of Energy, Energy Biosciences Division (DE-FG02-99ER20337A01) (to C. J. S.) and from the Biotechnology and Biological Sciences Research Council, UK (to V. E. F. T.). The costs of publication of this article were defrayed in part by the payment of page charges. This article must therefore be hereby marked "*advertisement*" in accordance with 18 U.S.C. Section 1734 solely to indicate this fact.

[S] The on-line version of this article (available at http://www.jbc.org) contains four supplementary time-lapse movies of actin filament severing.

¶ Supported by an Actions Thématiques et Incitives sur Programmes et Equipes from the CNRS.

** To whom correspondence should be addressed: Dept. of Biological Sciences, Purdue University, 333 Hansen Life Sciences Bldg., 201 S. University St., West Lafayette, IN 47907-2064. Tel.: 765-496-1769; Fax: 765-496-1496; E-mail: cstaiger@bilbo.bio.purdue.edu.

[1] The abbreviations used are: ABP, actin-binding protein; CP, capping protein; AtCP, *Arabidopsis* CP; AtVLN, *Arabidopsis* villin; DTT, dithiothreitol; G-actin, globular or monomeric actin; F-actin, filamentous actin; MmCP, mouse CP; PrABP80, *P. rhoeas* 80-kDa ABP; ZmPRO5, *Z. mays* profilin; SI, self-incompatibility; VHP, villin headpiece; ESI, electrospray ionization; MS, mass spectrometry; TOF, time-of-flight.

of actin filaments with reductions of 56 and 74% in pollen grains and pollen tubes, respectively (14). Because actin depolymerization is mimicked by treatments with calcium ionophores, attempts to model the response *in vitro* with known calcium-sensitive ABPs were made.

Pollen profilin binds to monomeric (G-) actin with a modest affinity and has increased G-actin sequestering activity in the presence of micromolar Ca^{2+} (14, 15). For native poppy profilin, however, the cellular concentration and apparent K_d at physiologically relevant [Ca^{2+}] are inconsistent with it functioning alone to mediate the depolymerization of actin. It was proposed that profilin acts in cooperation with other, yet to be discovered, ABPs to effect the destruction of actin networks during SI (14). Profilin acts like a simple sequestering protein in the presence of capping factors that block the barbed ends of filaments (16–18). The first example of this activity, associated with a heterodimeric capping protein from *Arabidopsis* (AtCP), has been reported recently (19). Alternatively, proteins that sever actin filaments could enhance profilin-mediated actin depolymerization. Indirect evidence for weak severing activity by ADF/cofilin makes this a potential candidate for SI, but other examples of efficient actin filament-severing proteins from plants are lacking (6).

Gelsolin, villin, and CapG comprise a family of related calcium-regulated ABPs that are found in many vertebrate and lower eukaryotic cells (20–22). Gelsolin is composed of six conserved 125–150-amino-acid gelsolin homology domains, designated G1–G6, and has Ca^{2+}-stimulated F-actin severing activity. Gelsolin also caps the barbed ends of actin filaments and nucleates formation of new filaments. Crystal structures for one or more of these gelsolin subdomains, coupled with spectroscopy and cryoelectron microscopy studies, have provided substantial insight about the molecular mechanisms of filament severing and capping (23). Villin has a core of six gelsolin subdomains but also contains an additional C-terminal actin-binding module called the villin headpiece (VHP) that allows it to make contact with two adjacent filaments and to cross-link filaments into bundles. In the presence of micromolar Ca^{2+} some, but not all, villins sever actin filaments and cap filament barbed ends (24, 25). Two actin-bundling proteins from lily pollen, 135-ABP and 115-ABP, are known (26–28), and sequence analyses reveal that both are plant villins (26, 29). Although lily villins bundle filaments in a Ca^{2+}-/calmodulin-dependent manner, they do not have severing or capping activity (30–32). The *Arabidopsis* genome contains sequences for five villin-like genes (*AtVLN1–5*; Refs. 6 and 33) but no gelsolin-only genes. A preliminary analysis of recombinant AtVLN1 demonstrates high affinity binding to F-actin and bundle formation but no severing or capping.[2]

Using affinity chromatography on DNase I-Sepharose, we identified an 80-kDa ABP from poppy pollen that is an efficient nucleator of actin filaments, has potent Ca^{2+}-stimulated severing activity, and regulates assembly by binding to filament barbed ends. *De novo* sequence determination by mass spectrometry indicates that ABP80 is related to gelsolin. This is the first direct evidence for a plant gelsolin and the first example of efficient actin filament-severing activity by a plant ABP.

EXPERIMENTAL PROCEDURES

Protein Purification—Approximately 5 g of pollen from field poppy (*P. rhoeas* L.) was hydrated at 37 °C for 30 min. Pollen was ground in a cooled mortar along with 1 g of fine sand (Sigma S-9887) in extraction buffer (1 M Tris, pH 7.5, 0.6 M KCl, 0.5 mM $MgCl_2$, 0.8 mM ATP, 1 mM DTT, 0.1 mM phenylmethylsulfonyl fluoride (34)) supplemented with a 1:100 dilution of protease inhibitors from a stock solution (2) for 30 min. The mixture was sonicated with five 30-s bursts, and Triton X-100 was added to 4% (v/v). The sonicate was clarified with three consecutive centrifugations of 30,000, 46,000, and 130,000 × *g*. The supernatant was passed through two layers of Miracloth (Calbiochem) and loaded onto a DNase I-Sepharose column (34) pre-equilibrated with Buffer G (1 mM Tris, pH 8.0, 0.2 mM ATP, 0.2 mM $CaCl_2$, 0.1 mM DTT, 0.005% NaN_3). The column was washed with Buffer G, and bound proteins were eluted with Ca^{2+}-free buffer G (1 mM Tris, pH 8.0, 0.2 mM ATP, 0.5 mM $MgCl_2$, 5 mM EGTA, 0.1 mM DTT, 0.005% NaN_3). Pooled protein fractions were dialyzed against Solution A (10 mM KCl, 1 mM DTT, 0.01% NaN_3, 10 mM Tris-HCl, pH 7.0, 1 mM phenylmethylsulfonyl fluoride, 1:200 protease inhibitors). The dialyzed protein was applied to a Q-Sepharose column (Amersham Biosciences) pre-equilibrated with Solution A, and bound proteins were eluted with a linear gradient of KCl (10–500 mM). The purified PrABP80 was dialyzed against Buffer G (2 mM Tris-HCl, pH 8.0, 0.01% NaN_3, 0.2 mM $CaCl_2$, 0.2 mM ATP, 0.2 mM DTT), aliquoted, frozen in liquid nitrogen, and stored at −80 °C. The protein was further clarified by centrifugation at 200,000 × *g* for 1 h before use. Protein concentration was determined with Bradford reagent (Bio-Rad) using bovine serum albumin as standard. PrABP80 from Q-Sepharose was probed with affinity-purified *Arabidopsis* VILLIN1 (AtVLN1) antibody at 1:100 dilution and developed as described previously (35). For production of recombinant AtVLN1, the first three gelsolin domains (G1–G3) of AtVLN1 (33) were amplified by PCR and cloned into pGEX-KG for the generation of a GST-VLN1(G1–G3) fusion protein. Alternatively, PrABP80 was probed with lily villin, 135-ABP serum kindly provided by T. Shimmen, Himeji Institute of Technology (28). Recombinant protein was purified from bacterial cells, and the glutathione *S*-transferase (GST) moiety was removed, according to the methods of Kovar *et al.* (36).

Actin was isolated from rabbit skeletal muscle acetone powder and purified by Sephacryl S-300 chromatography (37). Actin was labeled on Cys-374 with pyrene iodoacetamide (37). Mouse capping protein (MmCP; $\alpha_1\beta_2$ heterodimer) was kindly provided by D. R. Kovar (Yale University). *Zea mays* profilin (ZmPRO5) and AtCP were purified as described previously (15, 19). Human plasma gelsolin was expressed from a plasmid kindly provided by T. Pollard (Yale University) and purified from bacterial cells roughly according to Pope *et al.* (38) with DEAE-Sepharose and Cibacron Blue 3G-A chromatography.

Mass Spectrometry—For identification of PrABP80 by mass spectrometry, appropriate bands were excised from Coomassie-stained gels. The gel pieces were destained with 50% NH_4HCO_3, 50% CH_3CN. Supernatant was removed, and the gel pieces were dried under vacuum for 30 min. Gel pieces were reduced with 10 mM DTT in 100 mM NH_4HCO_3 at 56 °C for 45 min. Supernatant was removed and replaced with 55 mM C_2H_4INO for 30 min in the dark. Supernatant was removed again and replaced with 100 mM NH_4HCO_3 for 5 min and then diluted to 50% (v/v) CH_3CN for 15 min. Gel pieces were dried under vacuum for 30 min and digested with 0.01 mg/ml bovine pancreas trypsin (Sigma T-8658) for 45 min on ice. After removing the solution, gel pieces were incubated in digestion buffer (25 mM NH_4HCO_3; 5 mM $CaCl_2$) for 16 h. The digestion buffer was removed and saved, whereas the gel pieces were extracted with 25 mM NH_4HCO_3 for 15 min and then diluted to 50% (v/v) CH_3CN for an additional 15 min. This was followed by extraction with 5% CH_2O_2 for 15 min and then diluted to 50% (v/v) CH_3CN for an additional 15 min. This extraction step was repeated once. The washes were pooled with the digestion buffer. DTT was added to a final concentration of 1 mM, and the peptides were dried under vacuum. The peptides were resuspended in 20% $C_2HF_3O_2$, frozen in liquid N_2, and stored at −80 °C.

Poros Cleanup—An aliquot of the tryptic peptides was desalted in a glass purification capillary (Protana Engineering) using a 20-μm Poros R2 (polystyrene divinylbenzene; Applied Biosystems, Inc. (ABI), Foster City, CA). Briefly, the peptide mixture was loaded onto the R2 resin, washed three times with ~7 μl of 95:5, H_2O:ACN, 0.5% formic acid, and eluted with ~1.5 μl of 30:70, H_2O:ACN, 0.5% formic acid into a coated nanoelectrospray capillary (Protana).

Data Acquisition Parameters—Electrospray ionization (ESI) mass spectra were acquired using a QSTAR Pulsar *i* (ABI) quadrupole-TOF (time-of-flight) mass spectrometer equipped with a nano-ESI source (Protana). The ESI voltage was 1000 V, the TOF region acceleration voltage was 4 kV, and the injection pulse repetition rate was 6.0 kHz. External calibration was performed using porcine renin substrate decapeptide (Sigma), which yields doubly and triply charged monoisotopic signals (879.9705 and 586.9830, respectively). Mass spectra were acquired in an automated data-dependent mode (information-dependent acquisition) in positive mode over 25 min. *De novo* sequencing was performed with BioAnalyst software (ABI), and MS BLAST searches were performed at www.bork.embl-heidelberg.de.

[2] S. Huang, L. Blanchoin, T. Matsumoto, R. Robinson, and C. J. Staiger, unpublished data.

High Speed and Low Speed Co-sedimentation Assays—High and low speed co-sedimentation assays were used to examine the actin-binding and actin-cross-linking properties of PrABP80, respectively (36). In a 100-μl reaction volume, 2.0 μM G-actin alone, 200 nM PrABP80 alone, or G-actin with PrABP80 were incubated in 1× F-buffer (10× stock: 50 mM Tris-Cl, pH 7.5, 5 mM DTT, 5 mM ATP, 1 M KCl, 50 mM $MgCl_2$). These reactions were performed in the presence of 200 μM Ca^{2+} or 5 mM EGTA to give free Ca^{2+} of 180 μM and 15 nM, respectively. Free Ca^{2+} in the presence of EGTA was calculated with "EGTA" software by Petesmif (P. M. Smith, University of Liverpool, Liverpool UK), available at www.liv.ac.uk/~petesmif/software/egta.htm. After a 90-min incubation at 22 °C, samples were centrifuged at either 200,000 × *g* for 1 h at 4 °C or 13,500 × *g* for 30 min at 4 °C. Equal amounts of pellet and supernatant samples were separated by 12.5% SDS-PAGE.

Actin Nucleation Assay—Actin nucleation was carried out essentially as described by Schafer *et al.* (39). Monomeric actin at 2 μM (5% pyrene-labeled) was incubated with PrABP80 or AtCP for 5 min in Buffer G. Fluorescence of pyrene-actin was monitored with a PTI Alphascan spectrofluorimeter (Photon Technology International, South Brunswick, NJ) after the addition of 1/10 volume of 10× KMEI (1× contains 50 mM KCl, 1 mM $MgCl_2$, 1 mM EGTA, and 10 mM imidazole-HCl, pH 7.0). The number of ends (n) generated during the nucleation reaction was calculated from the slope of the polymerization curves at half-polymerization according to Equation 1,

$$\text{Slope} = k_+(\text{A})(n) - k_-(n) \qquad \text{(Eq. 1)}$$

where k_+ is the association rate constant at the pointed ends (1.3 μM^{-1} s^{-1}) (40), k_- is the dissociation rate constant (0.8 s^{-1}), and (A) is the concentration of actin monomers. These experiments were performed at 87 nM free Ca^{2+}, buffered with 1 mM EGTA, to minimize the effect of filament severing on the initial growth rates.

Elongation Assay to Determine the Affinity of PrABP80 for Actin Filaments—Various concentrations of PrABP80 or AtCP were incubated with 0.4 μM preformed actin filaments in KMI (50 mM KCl, 1 mM $MgCl_2$, 0.2 mM ATP, 0.2 mM $CaCl_2$, 0.5 mM DTT, 3 mM NaN_3 and 10 mM imidazole, pH 7.0) for 5 min at room temperature. The reaction mixture was supplemented with 1 μM G-actin (5% pyrene-labeled) saturated by 4 μM human profilin 1 to initiate actin elongation at barbed ends, and the final free $[Ca^{2+}]$ was 160 μM. The affinity of PrABP80 or AtCP for the barbed ends of actin filaments was determined by the variation of the initial rate of elongation as a function of the concentration of PrABP80 or AtCP using Equation 2

$$V_i = V_{if} + (V_{ib} - V_{if})\left(\frac{(K_d + [\text{ends}] + [\text{CP}] - \sqrt{(K_d + [\text{ends}] + [\text{CP}])^2 - (4[\text{ends}][\text{CP}])}}{2[\text{ends}]}\right) \qquad \text{(Eq. 2)}$$

where V_i is the observed rate of elongation, V_{if} is the rate of elongation when all barbed ends are free, V_{ib} is the rate of elongation when all barbed ends are capped, [ends] is the concentration of barbed ends, and [CP] is the concentration of capping protein or PrABP80. To test the effects of $[Ca^{2+}]$ on the affinity of PrABP80 for filament barbed ends, similar reactions were performed in the presence of 5 mM EGTA to give free $[Ca^{2+}]$ of 10 nM, 100 nM, 1 μM, and 10 μM. The data were modeled with Kaleidagraph v3.6 software (Synergy Software, Reading, PA).

Dynamics of Actin Filament Depolymerization—F-actin at 2.5 μM (40–50% pyrene-labeled) was depolymerized by the addition of an equimolar amount of ZmPRO5, in the presence or absence of PrABP80 or MmCP. The decrease in pyrene fluorescence accompanying actin depolymerization was monitored for 30 min after the addition of profilin. The final free $[Ca^{2+}]$ was 1 μM for most reactions. To test the requirement of Ca^{2+} for PrABP80-mediated depolymerization, free Ca^{2+} was reduced to 15 nM with 5 mM EGTA.

Fluorescence Microscopy of Actin Filaments—Individual actin filaments labeled with fluorescent phalloidin were imaged by fluorescence microscopy according to Blanchoin *et al.* (41, 42). To visualize actin filaments generated during nucleation, actin at 4 μM alone or together with PrABP80 were polymerized in 50 mM KCl, 1 mM $MgCl_2$, 1 mM EGTA, 0.2 mM ATP, 0.2 mM $CaCl_2$, 0.5 mM DTT, 3 mM NaN_3, and 10 mM imidazole, pH 7, at 25 °C for 30 min and labeled with an equimolar amount of rhodamine-phalloidin (Sigma) during polymerization. For these nucleation experiments, the free $[Ca^{2+}]$ was 87 nM. In other experiments, PrABP80 or AtCP were incubated, in the presence of 160 μM or 14.7 nM free Ca^{2+}, with prepolymerized rhodamine-phalloidin-labeled F-actin. The polymerized F-actin was diluted to 10 nM in fluorescence buffer containing 10 mM imidazole, pH 7.0, 50 mM KCl, 1 mM $MgCl_2$, 100 mM DTT, 100 μg/ml glucose oxidase, 15 mg/ml glucose, 20 μg/ml catalase, 0.5% methylcellulose. A dilute sample of 3 μl was applied to a 22 × 22 mm coverslip coated with poly-L-lysine (0.01%). Actin filaments were observed by epi-fluorescence illumination under a Nikon Microphot SA microscope equipped with a 60×, 1.4 NA Planapo objective, and digital images were collected with a Hamamatsu ORCA-ER 12-bit CCD camera using Metamorph 6.0 software.

In the elongation assay, actin filaments stabilized by rhodamine-phalloidin were elongated by actin monomers in presence of Alexa-488 phalloidin (Molecular Probes, Eugene OR) to stabilize the new filaments. Polymerization conditions were as given above for assembly from monomers, and the final free $[Ca^{2+}]$ was 76 nM.

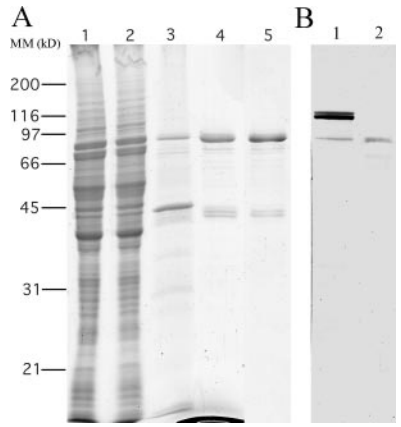

FIG. 1. **Purification of an 80-kDa polypeptide from poppy pollen.** *A*, Coomassie-stained gel. Poppy pollen extracts were fractionated on DNase I-Sepharose with elution by EGTA followed by binding to Q-Sepharose and elution with a linear salt gradient. The purified protein fraction has a major polypeptide of ~80 kDa and two minor contaminants of 42 and 40 kDa. The major protein is designated PrABP80. Loadings are as follows: *lane 1*, total extract (25 μg); *lane 2*, flow-through (25 μg); *lane 3*, DNase I-bound proteins (3 μg); *lane 4*, EGTA eluate (3 μg); *lane 5*, Q-Sepharose eluate (3 μg). The migration of molecular mass (*MM*) standards is given at the *left* in kDa. *B*, protein immunoblot probed with affinity-purified, anti-AtVLN1(G1–G3) antibody. *Lane 1*, poppy pollen total cell extract (30 μg); *lane 2*, purified PrABP80 (100 ng).

RESULTS

Purification of an 80-kDa P. rhoeas Actin-binding Protein (PrABP80)—To better understand the Ca^{2+}-mediated depolymerization of actin filaments in pollen, several independent approaches for the identification of ABPs are being pursued. During the purification of native actin from poppy pollen (14), we observed an ~80-kDa protein that bound to DNase I columns in the presence of 1 M salt. Because ABPs such as gelsolin, villin, and ADF form high affinity complexes with G-actin and are retained on DNase I-Sepharose columns (43–47), we sought to identify this putative pollen ABP. Hydrated poppy pollen was homogenized and clarified by differential centrifugation. The high speed supernatant (Fig. 1*A*, *lane 1*) was loaded onto DNase I-Sepharose, and most of the proteins passed into the flow-through (Fig. 1*A*, *lane 2*). After excessive buffer washes containing 200 μM Ca^{2+}, actin and a major 80-kDa protein remained on the DNase I-Sepharose column (Fig. 1*A*, *lane 3*). The 80-kDa protein and some of the actin (45 kDa) were eluted with EGTA (Fig. 1*A*, *lane 4*). Following dialysis, the 80-kDa protein was purified further by chromatography on Q-Sepharose, which removed most of the actin (Fig. 1*A*, *lane 5*). Typical samples contained a small amount of a 42-/40-kDa doublet, and the average purity of PrABP80 was greater than 80%.

Identification of PrABP80 as a Gelsolin-like Protein by Mass Spectrometry—To identify PrABP80, the polypeptide was isolated from Coomassie-stained polyacrylamide gels, digested with trypsin, and subjected to mass spectrometry (MS). Peptide mass fingerprinting with quadrupole-TOF yielded profiles that

TABLE I
PrABP80 peptides determined by ESI-MS/MS

	Peptide	Peptide MM[a]	*De novo* sequence determined by ESI-MS/MS[b]	Sequence matches[c]	Domain match[d]	135 ABP sequence ID	Human gelsolin sequence ID
	m/z	*Da*					
1	547.8	1093.6	L**AEVLQFF**K	ALEVIQFLK	G2	57%	11%
2	573.3	1144.6	LT**ELDTALA**AK	TVELDAVLGGR	G1	36%	27%
3	602.7	1804.9	YFMG**DSYLVLQT**SPGK	FYSGDSYIVLQTTAGK	G1	67%	38%
4	788.9	1575.8	V**STESSAFWHA**LGGK	EGTESSAFWFALGGK	G5	80%	20%
5	841.4	1680.8	VGAA**SDSYSTDGV**ALLR	KNLNDDTYVSDGIALIR	G5	41%	29%
6	856.9	1711.8	L**YQFDGENSNL**GAER	KIYQFNGANSNIQERAK	G2	44%	33%
7	923.9	1845.8	TVS**GGHDDVFLLDT**ENK	RTSLNHDDVFILDTEKK	G2	65%	35%

[a] MM, molecular weight.
[b] Letters are single amino acid code for fragments that were sequenced by tandem mass spectrometry (MS/MS). The presence of the putative b or y fragment ions (or both) (see Ref. 85 for fragment ion nomenclature) for boldface amino acid residues were observed in the experimental MS/MS spectrum and are within 175 ppm mass tolerance. Amino acid residues given in plain text did not fit these criteria.
[c] Sequences shown were the best match primary amino acid sequence from 135-ABP (GenBank accession number AAD54660). The entire *de novo* sequence was used in BLAST searches (dove.embl-heidelberg.de/Blast2/msblast.html).
[d] The gelsolin subdomain from which the best match was obtained (e.g. G1–G6) is given. These were determined by domain analysis of the 135-ABP sequence at SMART (smart.embl-heidelberg.de/).

matched villin/gelsolin proteins in current databases. To obtain sequence information, tryptic digests of PrABP80 were performed, and seven fragments were analyzed by ESI-MS/MS (Table I). The amino acid sequences were most similar to 135-ABP from lily pollen and *Arabidopsis* villins (Fig. 2). PrABP80 peptides shared 36–80% amino acid sequence identity with 135-ABP or AtVLN3, verifying that it is villin- or gelsolin-like. The peptides also shared 11–38% identity with human gelsolin. At 80 kDa, the purified protein is significantly smaller than the predicted M_r for plant villins, which range from 107,000 to 135,000. Moreover, none of the sequences obtained matched the C-terminal villin-headpiece for the known plant villins. Along with the biochemical properties (see below), these data suggest that PrABP80 is pollen gelsolin and not a villin-like protein.

The purified protein was recognized by an affinity-purified antibody (Fig. 1*B*, *lane 2*) raised against the G1–G3 domains of recombinant AtVLN1, suggesting that it is related to the gelsolin/villin family. It also cross-reacted with lily villin, 135-ABP antiserum (not shown). To demonstrate that PrABP80 exists within cells, a pollen extract was prepared by grinding ungerminated pollen under liquid nitrogen, and proteins were extracted with Laemmli buffer. Western blots using either antibody revealed a prominent pair of bands at ~135 kDa, as well as a distinct polypeptide of 80 kDa that comigrates with purified PrABP80 (Fig. 1*B*, *lane 1*). The higher M_r polypeptides are presumed to be similar to lily villins characterized by Shimmen and co-workers (26–32).

PrABP80 Binds to F-actin and Severs or Depolymerizes in a Ca^{2+}-dependent Manner but Does Not Have Filament Bundling Activity—The ability of PrABP80 to bind to F-actin was assayed with high speed co-sedimentation assays (Fig. 3*A*). The majority of the polymerized actin (F-actin) sedimented at 200,000 × *g* under these conditions (Fig. 3*A*, *lane 2*); however, no detectable PrABP80 sedimented in the absence of F-actin (Fig. 3*A*, *lane 10*). In the presence of F-actin and 15 nM free Ca^{2+}, a small amount of PrABP80 was found in the pellet (Fig. 3*A*, *lane 8*), indicating that PrABP80 can bind to the sides or ends of actin filaments. However, the amount of binding was modest when compared with side-binding proteins such as fimbrin (36) or AtVLN1 (not shown). In the presence of PrABP80 and 180 μM free Ca^{2+}, substantially more actin stayed in the supernatant (Fig. 3*A*, *lane 3*) when compared with the controls (Fig. 3*A*, *lanes 1* and *7*). This is consistent with Ca^{2+}-stimulated filament-severing or depolymerizing activity. Because this effect was observed at substoichiometric amounts of PrABP80 to actin, severing activity is the most plausible explanation.

Because all plant villins have the ability to bundle actin filaments, an activity that correlates with the presence of a VHP, we examined whether PrABP80 also has this property. To analyze bundling, low speed pelleting assays were performed (Fig. 3*B*). In the absence of PrABP80, very little F-actin sedimented at 13,500 × *g* (Fig. 3*B*, *lane 2*). A considerable amount of polymerized actin sedimented in the presence of AtVLN1 (Fig. 3*B*, *lane 6*); however, very little actin sedimented in the presence of PrABP80 (Fig. 3*B*, *lane 4*). The lack of PrABP80 filament bundling or cross-linking was confirmed by fluorescence microscopy, as described below. Unlike AtVLN1 or lily villins (28, 31), the 80-kDa ABP from poppy does not have bundling activity, which is consistent with it being a gelsolin-like protein.

PrABP80 Has Nucleation Activity—Gelsolin eliminates the lag period associated with initiation of actin assembly or nucleates actin filament formation (21, 22, 48). Experiments to examine the effect of PrABP80 on the dynamics of actin polymerization were performed. To minimize the potential effects of filament severing, these experiments were conducted in the presence of 1 mM EGTA to provide a free [Ca^{2+}] of 87 nM. As shown in Fig. 4*A*, when pyrene fluorescence was used to monitor rabbit muscle actin polymerization kinetically, the initial lag corresponding to the nucleation step decreased with increasing PrABP80 concentration. Similar results were observed with the heterodimeric capping protein from *Arabidopsis*, AtCP (Fig. 4*B*), as shown previously (19).

PrABP80 Inhibits the Addition of Profilin-Actin Complexes to Filament Barbed Ends—Gelsolin caps the newly created barbed end after it severs an actin filament (49). The activity of PrABP80 was also tested with a dynamic elongation assay from F-actin nuclei. The elongation rate depends on the availability of barbed ends, under these experimental conditions: 0.4 μM preformed F-actin was incubated with varying concentrations of ABP for 5 min, and polymerization was initiated with the addition of 1 μM G-actin (5% pyrene-labeled) at a free [Ca^{2+}] of 160 μM. The G-actin was saturated with 4 μM human profilin to prevent polymerization from pointed ends. The results showed that the initial elongation rate was decreased with substoichiometric amounts of PrABP80 (Fig. 5*A*), just like AtCP (19). By fitting the data to Equation 2 (see "Experimental Procedures"), an apparent K_d value for binding barbed ends of 5.5 nM was calculated (Fig. 5*B*). For comparison, a representative experiment with AtCP gave a K_d of 23 nM (Fig. 5*B*).

Similar experiments were performed in the presence of 5 mM EGTA and variable amounts of Ca^{2+} to examine the Ca^{2+} dependence of capping. Free Ca^{2+} between 10 nM and 10 μM

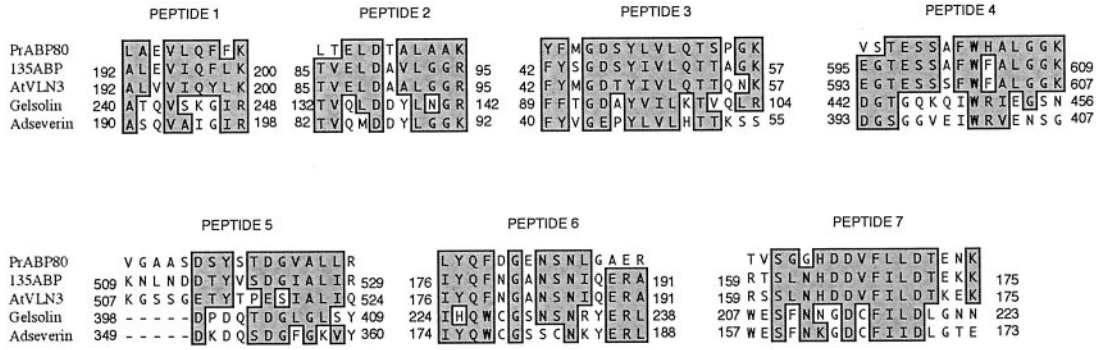

FIG. 2. **Sequence similarity between gelsolin/villin family members and the 80-kDa ABP.** Peptide sequences for PrABP80 from tryptic digests of gel-excised protein subjected to ESI-MS/MS were obtained as described under "Experimental Procedures." Alignments of the *de novo* sequences determined from seven fragments in comparison with other gelsolins and villins are shown. PrABP80 shares 36–80% amino acid sequence identity with corresponding regions of plant 135-ABP and 11–38% identity with human gelsolin (see Table I for additional information). Accession numbers are as follows: 135-ABP from *Lilium longiflorum* (AF088901), *Arabidopsis thaliana* VILLIN3 (AtVLN3; AF081203), human plasma gelsolin (CAA28000), and mouse adseverin (AAB61682). Alignments were created using the Clustal W algorithm with MacVector™ software (v7.1.1, Accelrys, Madison WI).

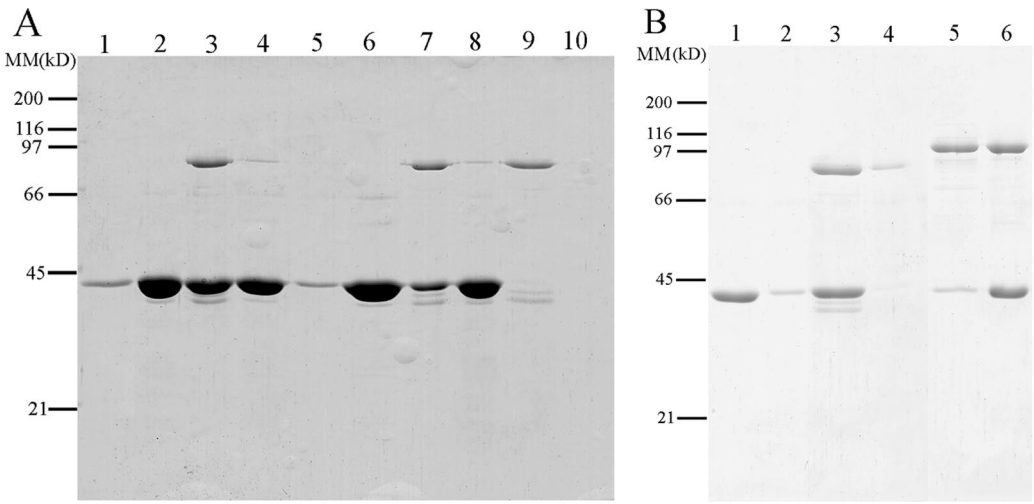

FIG. 3. **PrABP80 binds but does not cross-link actin filaments.** *A*, high speed co-sedimentation assays, in the presence or absence of calcium, were used to determine PrABP80 binding to F-actin. A mixture of F-actin (2 μM) and PrABP80 (0.2 μM) in the presence of 180 μM (high) or 15 nM (low) free Ca^{2+} was centrifuged at 200,000 $\times$ *g* for 1 h. The resulting supernatants and pellets were subjected to SDS-PAGE and Coomassie-stained. The samples include: *lane 1*, actin alone supernatant (high Ca^{2+}); *lane 2*, actin alone pellet (high Ca^{2+}); *lane 3*, actin plus PrABP80 supernatant (high Ca^{2+}); *lane 4*, actin plus PrABP80 pellet (high Ca^{2+}); *lane 5*, actin alone supernatant (low Ca^{2+}); *lane 6*, actin alone pellet (low Ca^{2+}); *lane 7*, actin plus PrABP80 supernatant (low Ca^{2+}); *lane 8*, actin plus PrABP80 pellet (low Ca^{2+}); *lane 9*, ABP80 alone supernatant; *lane 10*, PrABP80 alone pellet. *B*, a low speed co-sedimentation assay compared the filament bundling activity of PrABP80 with AtVLN1 (see Footnote 2). Actin alone, actin plus PrABP80, and actin plus AtVLN1 were incubated under polymerization conditions as in *panel A* except that the PrABP80 concentration was 0.8 μM and the reaction was centrifuged at 13,500 $\times$ *g*. Equivalent amounts of supernatant and pellet were separated by SDS-PAGE. Samples are: *lane 1*, actin alone supernatant; *lane 2*, actin alone pellet; *lane 3*, actin plus PrABP80 supernatant; *lane 4*, actin plus PrABP80 pellet; *lane 5*, actin plus AtVLN1 supernatant; *lane 6*, actin plus AtVLN1 pellet. The migration of molecular mass (*MM*) standards is given at the *left*.

had no effect on the affinity of PrABP80 for the barbed end of filaments (Table II). For PrABP80 binding to rabbit skeletal muscle actin, a K_d value of 2.74 nM at 10 μM free Ca^{2+} was not significantly different from the K_d of 2.02 nM at 100 nM Ca^{2+}. Identical experiments were conducted with recombinant human plasma gelsolin. Apparent K_d values ranged from 4.4 nM at low Ca^{2+} to 2.0 nM at 10 μM free Ca^{2+} (Table II). Therefore, PrABP80 and gelsolin binding to the barbed end of actin filaments is of high affinity and independent of Ca^{2+}.

PrABP80 Enhances Profilin-mediated Depolymerization of F-actin—The activity of PrABP80 was also measured with a dynamic depolymerization assay. The influence of PrABP80 and a capping protein (MmCP) on filament depolymerization was investigated by adding equimolar amounts of profilin (2.5 μM) to pyrene-labeled F-actin and monitoring the decrease in fluorescence. The results from a typical experiment in the presence of 1 μM free Ca^{2+} are shown in Fig. 6. The depolymerization rate was increased by substoichiometric amounts of PrABP80 (Fig. 6*A*, *bottom*), when compared with actin alone (Fig. 6*A*, *middle*). By comparison, the barbed end capping protein, mouse CP, inhibits profilin-mediated actin depolymerization (Fig. 6*A*, *upper*). To mimic the situation that occurs during the SI response of poppy, profilin-mediated depolymerization was performed with varying amounts of PrABP (1–10 nM) at high (1 μM) and low free Ca^{2+} (15 nM). The experiments in Fig. 6*B* show a dose-dependent, synergistic activity of PrABP and profilin that stimulates actin depolymerization. The results suggest that PrABP80 severs F-actin and produces additional ends for depolymerization. The observation that 10 nM PrABP80 in the presence of profilin caused nearly 50% depolymerization of F-actin is consistent with severing rather than monomer binding activity for the plant gelsolin. Moreover, this level of depolymerization was not observed when free calcium is reduced to 15 nM, a condition where PrABP80 should function like a barbed end cap (Fig. 6*B*, *top curve*). Indeed, at low calcium, PrABP

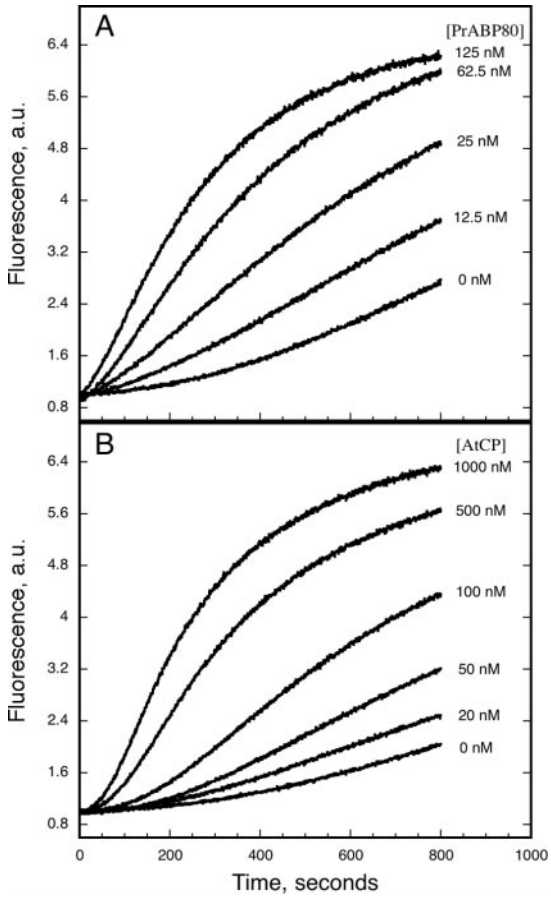

FIG. 4. **PrABP80 nucleates filament assembly from monomers.** PrABP80 and AtCP at various concentrations were incubated for 5 min with 2 μM actin (5% pyrene-labeled) prior to polymerization. Pyrene fluorescence (arbitrary units, *a.u.*) was plotted *versus* time after the addition of polymerization salts to initiate polymerization. *A*, PrABP80 at various concentrations, from *bottom* to *top*: 0, 12.5, 25, 62.5, and 125 nM. *B*, AtCP at various concentrations, from *bottom* to *top*: 0, 20, 50, 100, 500, and 1000 nM.

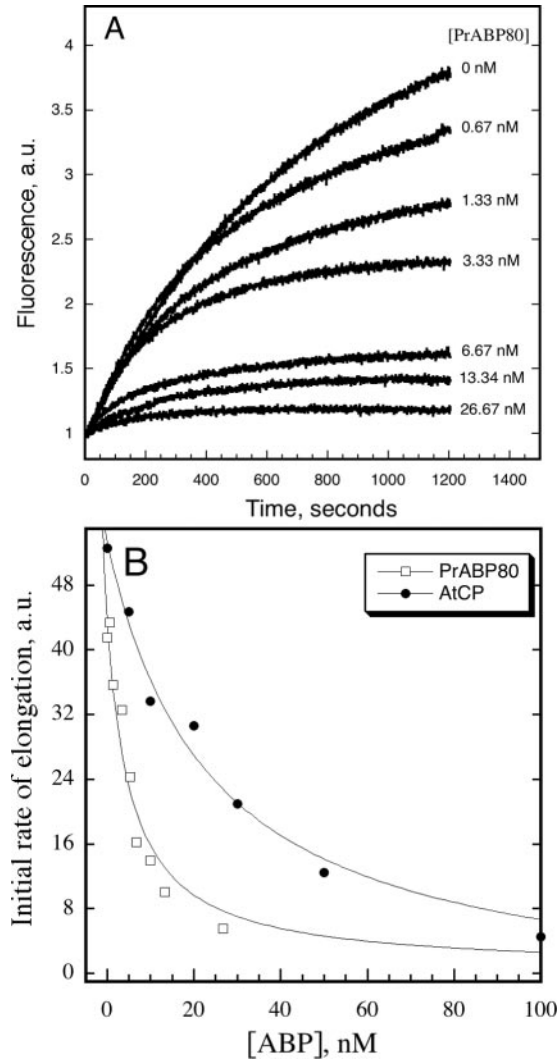

FIG. 5. **Elongation of actin filaments by the addition of profilin-actin complex to barbed ends is inhibited by PrABP80.** *A*, preformed F-actin (0.4 μM) was incubated with different concentrations of PrABP80. To initiate actin elongation at the barbed end, 1 μM G-actin saturated with 4 μM human profilin I was added to each reaction. The change in pyrene-actin fluorescence accompanying polymerization was plotted *versus* time after the addition of G-actin. From *bottom* to *top*, PrABP80 concentration is: 26.67, 13.34, 6.67, 3.33, 1.33, 0.67, and 0 nM. *a.u.*, arbitrary units. *B*, initial rates of polymerization *versus* PrABP80 (*open squares*) and AtCP (*closed circles*) concentration were plotted for the experiment in *panel A*. The data were fit with Equation 2 (see "Experimental Procedures") to determine apparent binding constant values of 5.5 nM for PrABP80 and 23 nM for AtCP.

inhibited actin depolymerization relative to the control of actin and profilin alone. The severing activity was confirmed by measuring the lengths of prepolymerized rhodamine-stabilized actin filaments incubated with PrABP80 and by a time course of individual actin filaments severed by PrABP80.

Effects of PrABP80 on Actin Filament Length—Fluorescence microscopy was used to determine the effect of PrABP80 on the length distribution of actin filaments. When 4 μM actin was polymerized in the presence of an equimolar amount of rhodamine-phalloidin and diluted to a final concentration of 10 nM before attaching to polylysine-coated coverslips, the number of filaments per field was few, and their length distribution was approximately exponential (Fig. 7*A*; mean of 7.5 $\pm$ 5.1 μm). By contrast, when actin was polymerized in the presence of 9.4 (Fig. 7*B*), 18.8 (Fig. 7*C*), 47 (Fig. 7*D*), 94 (Fig. 7*E*), and 188 nM PrABP80 (Fig. 7*F*), the mean length of filaments was 3.2 $\pm$ 2.1, 2.9 $\pm$ 2.1, 1.4 $\pm$ 1.0, 1.0 $\pm$ 0.9, and 0.7 $\pm$ 0.6 μm ($n \geq 178$), respectively. These results demonstrate that PrABP80 reduced actin filament length in a dose-dependent manner. This is consistent with PrABP80 blocking assembly at barbed ends, inhibiting filament annealing, as well as increasing the number of actin filaments during assembly by nucleation. Similar results are observed with AtCP and mouse CP (19). There was no evidence for the formation of bundles or cross-linked networks in the presence of PrABP80, which would be expected if it exhibited villin-like activity.

We confirmed that the barbed ends of actin filaments are blocked by PrABP80 using a fluorescence microscope assay for filament elongation. Actin filaments labeled with rhodamine-phalloidin (Fig. 8, *red*) were used as prelabeled templates for subsequent elongation. The elongation was performed in the presence of Alexa-488 phalloidin so that newly elongated actin filaments were labeled green. As a control, when both ends are free, green actin elongated from both ends of red actin filaments (Fig. 8*A*). New growth under these conditions was asymmetric; the presumed barbed end typically had a long stretch of green filament, whereas the pointed end had a comparatively short length of green filament. In the presence of saturating amounts of PrABP80 (Fig. 8*C*) or AtCP (Fig. 8*B*), green actin filaments grew almost exclusively from one end of the red actin filaments. Moreover, the extent of green actin filament growth was short, suggesting that PrABP80 blocked all available

TABLE II
PrABP80 affinity for barbed ends is not Ca^{2+}-sensitive

$[Ca^{2+}]_{free}$ [a]	PrABP80 (K_d ± S.D.)	GS (K_d ± S.D.)
	n [b]	
10 nM	6.44 ± 4.17 nM (7)	4.40 ± 1.58 nM (7)
100 nM	2.02 ± 0.57 nM (8)	1.64 ± 0.57 nM (8)
1 μM	4.05 ± 1.51 nM (7)	2.67 ± 1.40 nM (8)
10 μM	2.74 ± 1.36 nM (7)	2.00 ± 0.79 nM (8)

[a] Free calcium concentration was calculated using the "EGTA" program.
[b] Mean K_d values (in nM) for binding to filament barbed ends from a representative experiment (±S.D.) of the elongation assay performed at different free calcium levels are given. Sample size (n) for these experiments is the number of PrABP80 and human plasma gelsolin (GS) concentrations used to determine a K_d value.

barbed ends and green actin filaments extended only from pointed ends.

PrABP80 Severing Activity Can Be Observed with Fluorescence Microscopy—Gelsolin is able to sever phalloidin-stabilized F-actin (50). Initially, we tested whether PrABP80 can sever populations of prepolymerized F-actin stabilized with rhodamine-phalloidin. As shown in Fig. 9, PrABP80 significantly reduced the length of actin filaments (mean = 0.4 ± 0.4 μm) after incubation in the presence of 160 μM free Ca^{2+} for 30 min (Fig. 9*D*) when compared with controls (Fig. 9*A*, mean = 5.1 ± 3.7 μm). After incubation with 500 nM AtCP (Fig. 9*B*), the mean length of actin filaments, 4.9 ± 3.4 μm, was not significantly different from the control. The reduction in filament length by PrABP80 was dependent on Ca^{2+}; reactions performed in the presence of 5 mM EGTA and 16 nM free Ca^{2+} had a mean filament length of 4.7 ± 3.2 μm (Fig. 9*C*). These results indicated that PrABP80 not only caps ends but also severs actin filaments.

The severing activity of PrABP80 was also demonstrated by monitoring the time course of actin filament length reduction directly. As shown in Fig. 10, the number of breaks (*arrows*) in a field of actin filaments increased over time (see also Supplemental Data; Movies 1–4). In the absence of PrABP80, a minimal amount of photobleaching was observed, but filaments were not severed or reduced in length (not shown). Many of the breaks caused by PrABP80 were associated with the presence of a kink or bend in the filament backbone, as shown previously for gelsolin by electron microscopy and light microscopy (50, 51). This provided convincing and direct evidence that PrABP80 can sever F-actin.

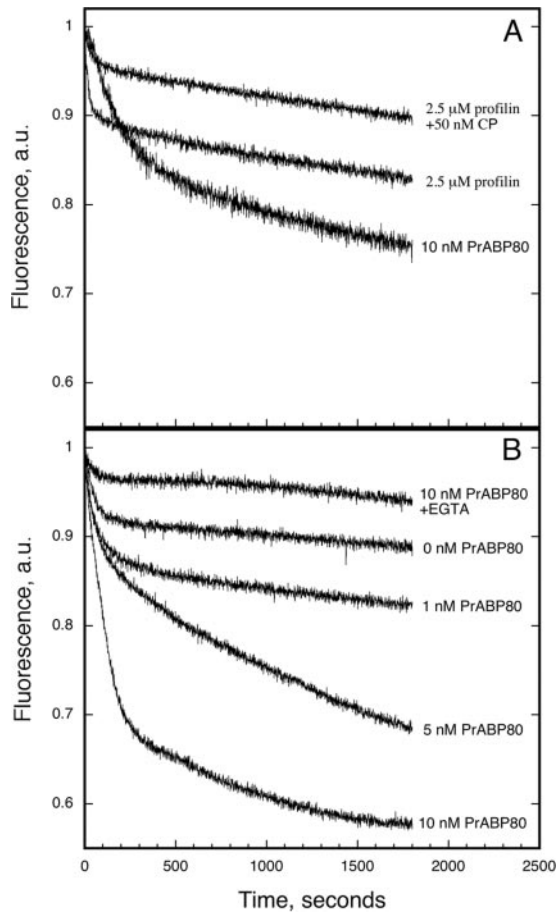

FIG. 6. **PrABP80 enhances profilin-mediated actin filament depolymerization.** ZmPRO5 (2.5 μM) alone, or ZmPRO5 together with MmCP or PrABP80, was added to F-actin solutions prepared from 2.5 μM actin (40–50% pyrene-labeled). Depolymerization was recorded by reduction in pyrene fluorescence beginning from the addition of protein at time = 0. Except where noted, all reactions were performed in the presence of 1 μM free Ca^{2+}. *A*, in addition to 2.5 μM F-actin, the reactions contained: 2.5 μM profilin + 50 nM CP, 2.5 μM profilin, or 10 nM PrABP80, as given on the figure. *a.u.*, arbitrary units. *B*, all reactions contained 2.5 μM actin in polymer, to which 2.5 μM profilin and variable amounts of PrABP80 were added. As noted on the figure, experiments included: 10 nM PrABP80 in the presence of 15 nM free Ca^{2+} (+EGTA), no PrABP80, 1 nM PrABP80, 5 nM PrABP80, and 10 nM PrABP80.

DISCUSSION

Here we report the first molecular, biochemical, and cytological evidence for the existence of a gelsolin-like protein in plants. An 80-kDa polypeptide from *P. rhoeas* pollen was purified to near homogeneity, and its sequence was determined by mass spectrometry. A combination of recognition by an affinity-purified AtVLN antibody and *de novo* sequence determination identified PrABP80 as gelsolin or villin-like. Gelsolin (80–90 kDa) is a calcium- and phosphoinositide-regulated actin cytoskeleton remodeling protein identified originally from alveolar macrophages (52). Gelsolin has three main activities (21, 48, 53): it binds along the backbone of actin filaments and severs the contacts between adjacent subunits; it caps the barbed end of F-actin with high affinity, thereby preventing subunit addition and loss from the capped end; and it associates with two or three actin subunits to nucleate assembly of new filaments. We have demonstrated that, like vertebrate gelsolin, PrABP80 has a high affinity for filament barbed ends, nucleates filament formation during assembly, severs existing filaments, and stimulates actin depolymerization. However, unlike plant or non-plant villins, it does not bundle F-actin. The molecular weight, sequence, and biochemical activities, as well as direct demonstration of severing activity by fluorescence microscopy, provide overwhelming evidence that PrABP80 is a plant gelsolin.

Kinetic analyses of PrABP80 interaction with pyrene-labeled actin demonstrated that substoichiometric amounts of PrABP80 eliminate the initial lag period required for actin assembly from monomers and prevent the addition of profilin-actin complexes onto actin filament ends. These properties are consistent with high affinity binding and capping of filament barbed ends. Indeed, when a titration with ABP was used to calculate an apparent K_d for barbed ends, PrABP80 has a value of 2–6 nM. The binding constant of gelsolin family members for capping barbed ends may be as low as 10 pM for platelet gelsolin in the presence of 150 μM Ca^{2+} (54), but more typical values range from 1 to 40 nM (55–58). The ability of PrABP80 to block subunit addition at the barbed end of filaments was confirmed by fluorescence microscopy. In a two-color filament elongation assay (41), limited green filament growth was observed from only one end of pre-existing red filaments in the presence of PrABP80, whereas controls

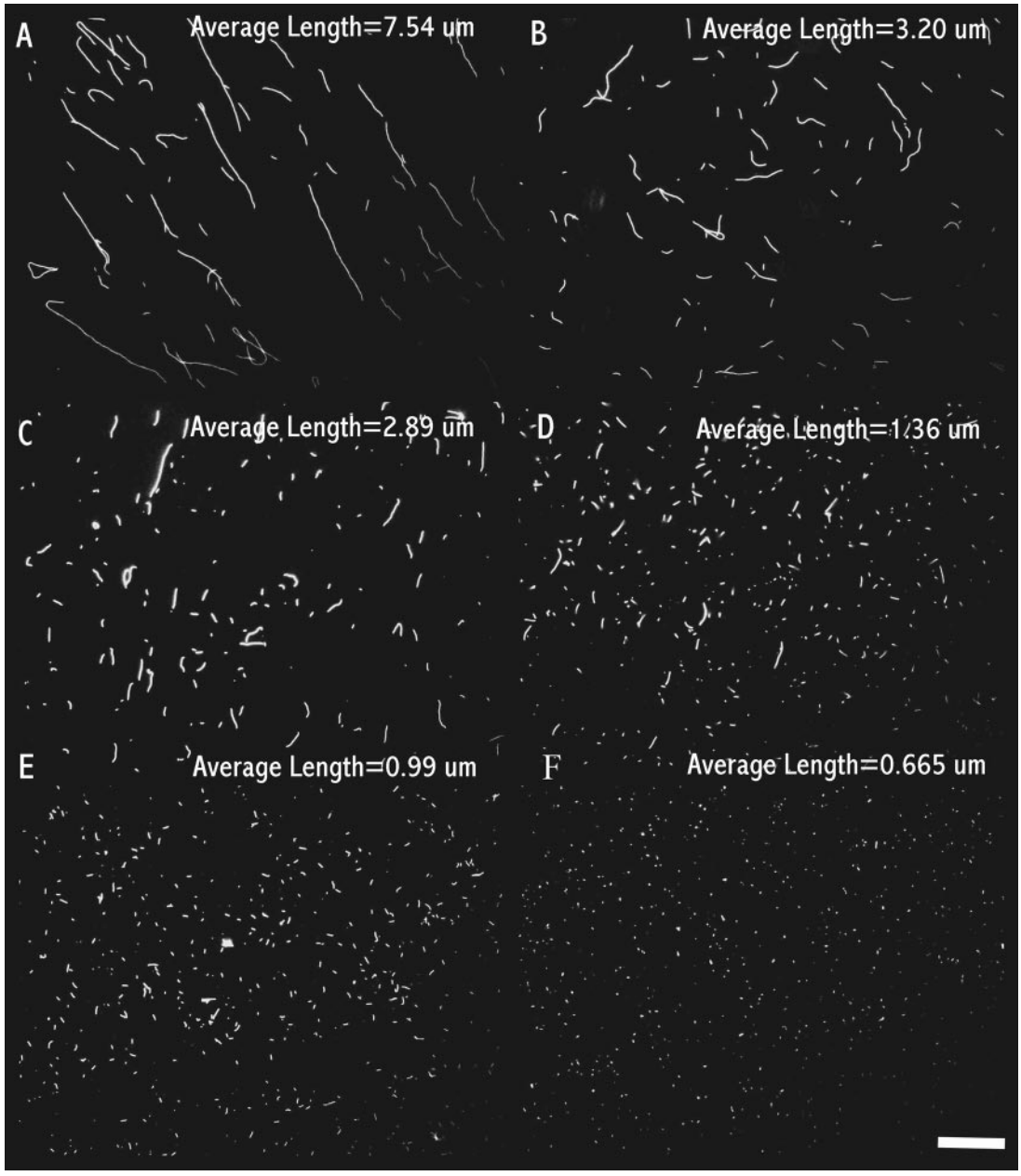

FIG. 7. **PrABP80 reduces filament length during assembly from monomeric actin.** Fluorescence micrographs of individual actin filaments assembled in the presence or absence of PrABP80 are shown. The effect of PrABP80 on filament length is shown. In each case, 4 μM Mg-ATP-actin was polymerized for 30 min in the presence of 4 μM rhodamine-phalloidin. Average filament lengths were determined from measurement of at least 100 filaments. *A*, actin filaments formed in the absence of PrABP80 or in the presence of 9.4 nM (*B*), 18.8 nM (*C*), 47 nM (*D*), 94 nM (*E*), and 188 nM PrABP80 (*F*). The *scale bar* in *panel F* represents 10 μm.

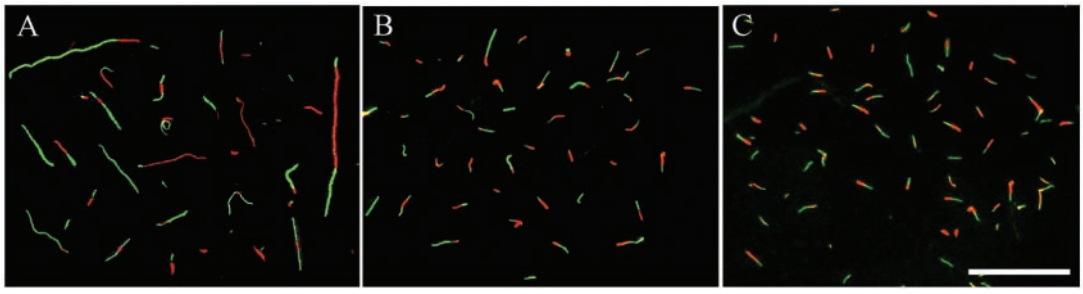

FIG. 8. **Elongation of actin filaments from the barbed end is blocked by PrABP80.** Two-color overlays of actin filament assembly from rhodamine-phalloidin-labeled actin template (*red*). The new growth is marked by Alexa-488 phalloidin (*green*). *A*, 2 μM F-actin stabilized with rhodamine-phalloidin was incubated with 1 μM Mg-ATP-actin for 15 min in the presence of 1 μM Alexa-488 phalloidin. Because the filament density was somewhat lower, due to the increased filament length at equivalent actin concentrations to those shown in *panels B* and *C*, this image is a montage created from three different fields. *B*, AtCP-capped actin filaments (0.5 μM) labeled with rhodamine-phalloidin were used for new polymerization as described for *panel A*. *C*, PrABP80-capped actin filaments (100 nM) were used for polymerization. The *scale bar* in *panel C* represents 10 μm.

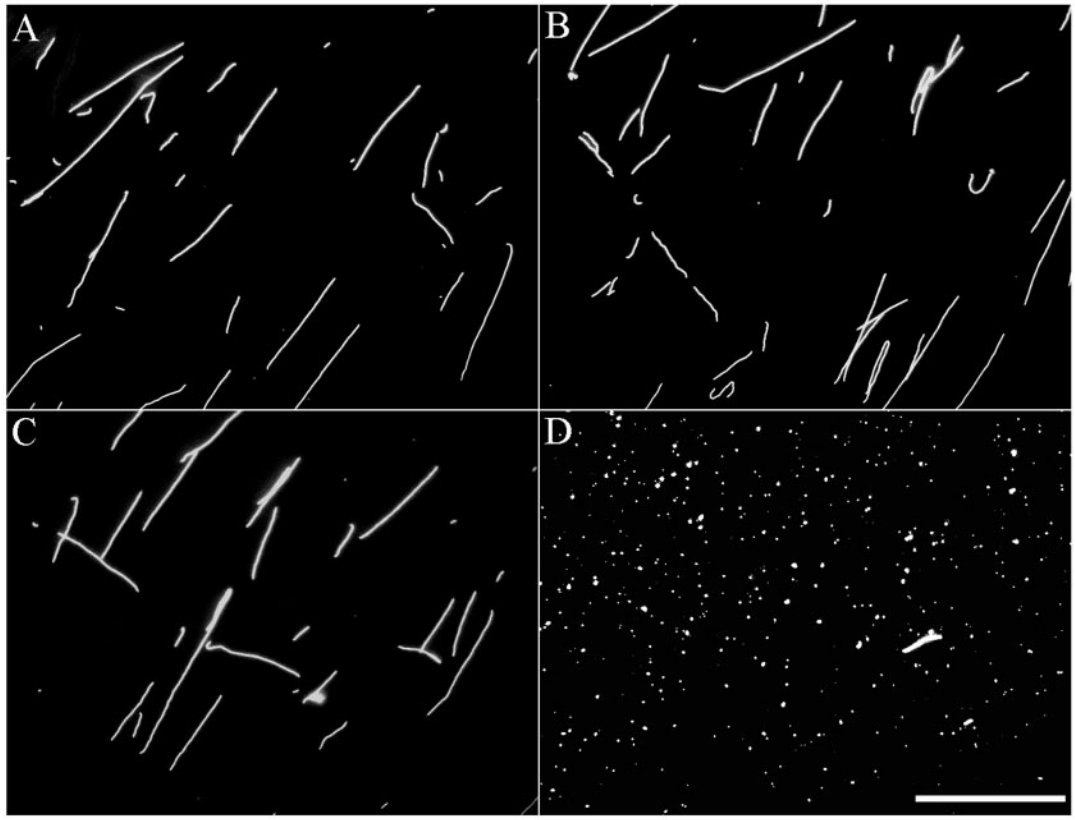

FIG. 9. **The length of preformed filaments is reduced in the presence of PrABP80.** Actin filaments (4 μM) labeled with rhodamine-phalloidin were incubated with AtCP or PrABP80, and images were collected after a 30-min incubation. PrABP80 reduces the mean length of actin filaments in a Ca^{2+}-dependent manner. *A*, actin alone; *B*, actin + 500 nM AtCP; *C*, actin + 166 nM PrABP80 in the presence of 14.7 nM free Ca^{2+}; and *D*, actin + 166 nM ABP80 in the presence of 160 μM Ca^{2+}. *Bar* = 10 μm.

showed growth from both ends, and one new section of filament was typically much longer than that extending from the other end.

The actin-binding activity of gelsolin is typically held to be Ca^{2+}-regulated, but the details of this regulation are complex and somewhat controversial. Part of the complexity is due to the fact that an individual gelsolin polypeptide can bind multiple Ca^{2+} molecules and additional sites are coordinated with bound actin. Type-2 sites reside wholly within the gelsolin polypeptide, whereas type-1 sites require residues on both gelsolin and a bound actin. X-ray crystallographic studies indicate that gelsolin has up to six type-2 sites, one for each gelsolin-homology domain, and two type-1 sites (59–62). In the absence of Ca^{2+}, the six homologous domains are folded into a compact, globular structure with the actin-binding sites buried (63). An overwhelming amount of biochemical and structural data lend support to a "tail latch" mechanism, whereby calcium binding induces a conformational change that releases the C-terminal helix of G6 from its contact with G2 and exposes the actin-binding site(s) (60, 62–66). However, there is some dispute about the level of Ca^{2+} required to undo the structural restraint. Using dynamic light scattering, Pope *et al.* (38) provide evidence for conformational changes at nanomolar Ca^{2+} levels, whereas Lin *et al.* (66) use endogenous tryptophan fluorescence to show that unlatching requires micromolar Ca^{2+}. Several studies report that the capping activity of gelsolin and villin is activated half-maximally at 10–30 nM Ca^{2+}, whereas severing activity requires micromolar Ca^{2+} for full activation (67, 68). Here, we find that PrABP80 has substantial capping and nucleating activity at 10–100 nM free Ca^{2+}, consistent with unlatching and/or activation at these physiological levels of Ca^{2+}. Moreover, the apparent K_d value for binding filament barbed ends does not change significantly over the range of 100 nM to 10 μM Ca^{2+}, levels that are found in actively growing and stimulated pollen tubes (69, 70). This suggests that within pollen, much of the PrABP80 will be bound to the ends of actin filaments. An alternative model for the lack of Ca^{2+} regulation would be that PrABP80 is missing the latch helix or G6 domain. Creation of a mutant human plasma gelsolin that lacks just 3% of the C-terminal amino acid sequence alleviates Ca^{2+} regulation (65). This theory is consistent with the molecular weight of PrABP80 and the presence of splice variants in other plants that comprise just G1–G5. Further understanding of this phenomenon will require additional biochemical studies and isolation of a full-length cDNA for PrABP80.

Several lines of investigation provide evidence for actin filament severing by PrABP80. The rate of depolymerization of pre-existing filaments by profilin is rather limited on its own and is inhibited by barbed end capping factors. However, by creating new ends, severing proteins enhance profilin-mediated actin filament disassembly. Substoichiometric amounts of PrABP80 increased the depolymerization rate of pyrene-labeled actin filaments in a dose- and Ca^{2+}-dependent manner. Fluorescence microscopy also showed that PrABP80 can reduce the mean length of pre-assembled actin filaments in a Ca^{2+}-dependent manner. The most compelling and direct evidence for severing comes from time-lapse movies of individual filaments in the presence of PrABP80 (see Supplemental Data; Movies 1–4). Rhodamine-phalloidin-stabilized actin filaments developed numerous breaks along their backbone after just seconds of incubation with PrABP80.

To date, only limited and circumstantial evidence for sever-

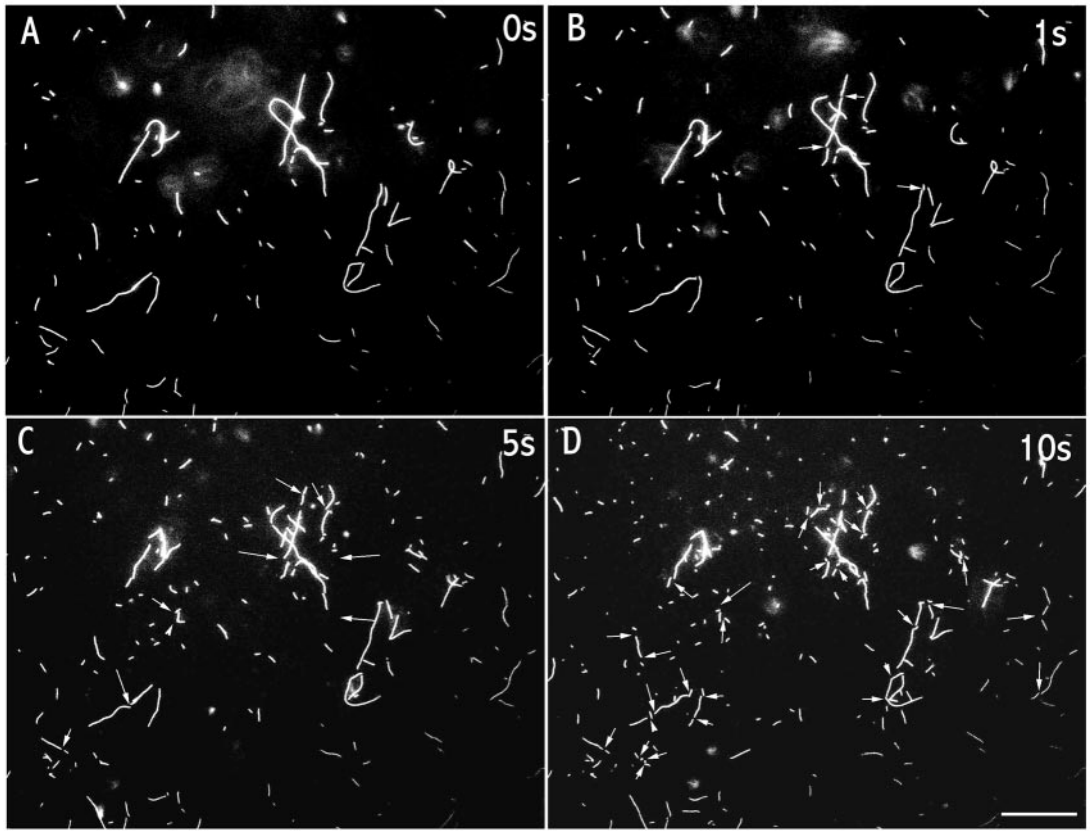

FIG. 10. **Severing activity of PrABP80 is observed directly by fluorescence microscopy.** Prepolymerized, rhodamine-phalloidin-labeled actin filaments were incubated with PrABP80, and images were collected every 500 ms. Individual filaments showed an increasing number of breaks (*arrows*) as time elapsed, consistent with severing activity. Many of the breaks occurred at bends in the filament. See Supplemental Data, Movie 1, for a QuickTime movie of the entire time series.

ing activity by plant ABPs exists in the literature. Weak severing activity is known for non-plant ADF/cofilin proteins (71). Severing has never been demonstrated directly for a plant ADF, although it is often inferred from depolymerization and polymerization assays (72, 73). The relative contribution of severing *versus* enhancing the off-rate at pointed ends to ADF/cofilin depolymerizing activity remains controversial (74–76). There is limited biochemical evidence for a Ca^{2+}-dependent ABP from *Mimosa pudica*, the sensitive plant, that is related to gelsolin/fragmin-like proteins (77). When extracts of mimosa plants were applied to a DNase I column in the presence of Ca^{2+}, two polypeptides, a major protein of 42 kDa and a less abundant 90-kDa protein, were eluted with EGTA. After EGTA was removed, the eluate increased the amount of actin in the supernatant by sedimentation analysis and generated short actin filaments as assessed by electron microscopy. Moreover, the two proteins facilitated actin polymerization from monomers in the presence of 200 μM Ca^{2+} and decreased the lag period for assembly. These properties are diagnostic for either actin capping or severing proteins. However, depolymerization assays or direct analysis of severing to distinguish between these possibilities were not performed. The 42-kDa protein has limited sequence similarity with *Arabidopsis* and lily villins, with one of four peptides sharing 31–46% identity. However, the three other peptide sequences failed to align with plant villins.

The biochemical evidence for a plant gelsolin is somewhat surprising, based solely on analysis of the *Arabidopsis* genome data base (6, 78). Although both gelsolin and villin are constructed from the same core of six tandem gelsolin subdomains, villin contains an additional actin-binding module (20, 21). This 8.5-kDa VHP confers Ca^{2+}-independent actin bundling activity upon the villin family members, a biochemical property that is missing from gelsolins. All five gelsolin/villin-related genes in *Arabidopsis* (*AtVLN1–5*) contain a VHP, suggesting that they encode villin-like proteins (6, 33). Gelsolin could be generated as an alternative splicing product from any of the AtVLN transcripts. Indeed evidence for a CapG-like splice variant for AtVLN1 (33)[2] and a G1–G5 protein from AtVLN3 (GenBank™ accession number AY093052) exists in current databases.

The role of gelsolin in plant cells could include the regulation of filament dynamics in response to fluxes in calcium or PPIs. In pollen tubes, a tip high oscillatory gradient of $[Ca^{2+}]_i$ is essential for tip growth (69, 70, 79, 80). A remarkable correspondence between actin organization at the tips of pollen tubes, the $[Ca^{2+}]_i$ gradients, and evidence for oscillatory actin dynamics (81), suggest a role for actin dynamics in apical tip growth (82). A Ca^{2+}-stimulated actin filament-severing protein, such as PrABP80, could act as a sensor for the oscillating $[Ca^{2+}]_i$ and contribute to the creation of a dynamic population of actin filaments at the apex of pollen tubes. Several groups have invoked gelsolin-like activities for Ca^{2+}-mediated actin rearrangements in response to ionophores or extracellular signals (13, 83, 84). The identification of PrABP80 lends some credence to these hypotheses, but further experimentation is required to verify that this particular class of ABP is involved in actin reorganization during each of these responses.

Actin depolymerization is a hallmark of the SI response of field poppy and can be mimicked by drugs that raise $[Ca^{2+}]_i$ (13, 14). The rapid and sustained 50–80% reduction in polymer levels is unrivaled by most eukaryotic cells. Reconstitution experiments with native pollen profilin, a G-actin-binding pro-

tein that has increased sequestering activity at elevated Ca^{2+}, fail to account for the level of depolymerization observed *in vivo* (14). We proposed previously that profilin acts in cooperation with other ABPs to mediate this depolymerization. Two proteins, capping protein (19) and PrABP80, may be such partners of profilin. The former is predicted to assist profilin in maintaining a large pool of unpolymerized actin by blocking assembly of the profilin-actin complex onto filament barbed ends and allowing profilin to function as a simple actin sequestering protein (18). PrABP80 could also assist filament depolymerization by Ca^{2+}-activated severing and the creation of new pointed ends for depolymerization by profilin. The feasibility of this mechanism is supported by experiments in which equimolar amounts of profilin were added to pre-existing actin filaments along with nM amounts of PrABP80. Up to 50% actin depolymerization was observed with just 10 nM PrABP80, but only in the presence of μM free Ca^{2+}. This is remarkably similar to the situation that occurs during SI. To test this molecular model thoroughly, we will need to determine the cellular concentrations for CP and PrABP80 in pollen, measure their affinity for plant actin filament ends, and determine the efficiency of severing at various physiological [Ca^{2+}].

In summary, we have obtained the first direct evidence for a gelsolin-like protein in plants. Our characterization of PrABP80 provides the first demonstration of efficient Ca^{2+}-regulated severing activity for a plant ABP. PrABP80 also caps the barbed ends of actin filaments with high affinity in the presence or absence of Ca^{2+} and can nucleate filament assembly from monomers. Its properties suggest that PrABP80 may assist profilin with Ca^{2+}-mediated depolymerization of actin filaments during SI in poppy.

Acknowledgments—Microscopy facilities were established with partial support from the National Science Foundation (0217552-DBI). We recognize the Mass Spectrometry Consortium for the Life Sciences at the University of Minnesota and various supporting agencies, including the National Science Foundation for Grant 9871237-MRI used to purchase the MS instruments. We gratefully acknowledge the help and advice from members of the Purdue Motility Group and thank D. R. Kovar (Yale University) and A. McGough (Purdue) for critical review of the manuscript. We also thank T. Pollard (Yale University) for providing the human plasma gelsolin clone and T. Shimmen (Himeji Institute, Japan) for the antibody against 135-ABP.

REFERENCES

1. Liu, X., and Yen, L.-F. (1992) *Plant Physiol.* **99,** 1151–1155
2. Ren, H., Gibbon, B. C., Ashworth, S. L., Sherman, D. M., Yuan, M., and Staiger, C. J. (1997) *Plant Cell* **9,** 1445–1457
3. Honys, D., and Twell, D. (2003) *Plant Physiol.* **132,** 640–652
4. Yokota, E., and Shimmen, T. (2000) in *Actin: A Dynamic Framework for Multiple Plant Cell Functions* (Staiger, C. J., Baluska, F., Volkmann, D., and Barlow, P., eds) pp. 103–118, Kluwer Academic Publishers, Dordrecht, The Netherlands
5. Vidali, L., and Hepler, P. K. (2001) *Protoplasma* **215,** 64–76
6. Staiger, C. J., and Hussey, P. J. (2004) in *The Plant Cytoskeleton in Cell Differentiation and Development* (Hussey, P. J., ed) pp. 32–80, Blackwell Publishers, UK
7. Hepler, P. K., Vidali, L., and Cheung, A. Y. (2001) *Annu. Rev. Cell Dev. Biol.* **17,** 159–187
8. Gibbon, B. C., Kovar, D. R., and Staiger, C. J. (1999) *Plant Cell* **11,** 2349–2363
9. Vidali, L., McKenna, S. T., and Hepler, P. K. (2001) *Mol. Biol. Cell* **12,** 2534–2545
10. Franklin-Tong, V. E., Ride, J. P., Read, N. D., Trewavas, A. J., and Franklin, F. C. H. (1993) *Plant J.* **4,** 163–177
11. Franklin-Tong, V. E., Hackett, G., and Hepler, P. K. (1997) *Plant J.* **12,** 1375–1386
12. Franklin-Tong, V. E. (1999) *Plant Cell* **11,** 727–738
13. Geitmann, A., Snowman, B. N., Emons, A. M. C., and Franklin-Tong, V. E. (2000) *Plant Cell* **12,** 1239–1251
14. Snowman, B. N., Kovar, D. R., Shevchenko, G., Franklin-Tong, V. E., and Staiger, C. J. (2002) *Plant Cell* **14,** 2613–2626
15. Kovar, D. R., Drøbak, B. K., and Staiger, C. J. (2000) *Plant Cell* **12,** 583–598
16. Pantaloni, D., and Carlier, M.-F. (1993) *Cell* **75,** 1007–1014
17. Perelroizen, I., Didry, D., Christensen, H., Chua, N.-H., and Carlier, M.-F. (1996) *J. Biol. Chem.* **271,** 12302–12309
18. Kang, F., Purich, D. L., and Southwick, F. S. (1999) *J. Biol. Chem.* **274,** 36963–36972
19. Huang, S., Blanchoin, L., Kovar, D. R., and Staiger, C. J. (2003) *J. Biol. Chem.* **278,** 44832–44842
20. Friederich, E., and Louvard, D. (1999) in *Guidebook to the Cytoskeletal and Motor Proteins* (Kries, T., and Vale, R., eds) 2nd Ed., pp. 175–179, Oxford University Press, New York
21. Yin, H. L. (1999) in *Guidebook to the Cytoskeletal and Motor Proteins* (Kreis, T., and Vale, R., eds) Vol. 2nd Ed., pp. 99–102, Oxford University Press, New York
22. Kwiatkowski, D. J. (1999) *Curr. Opin. Cell Biol.* **11,** 103–108
23. McGough, A. M., Staiger, C. J., Min, J.-K., and Simonetti, K. D. (2003) *FEBS Lett.* **552,** 75–81
24. Glenney, J. R., Jr., Bretscher, A., and Weber, K. (1980) *Proc. Natl. Acad. Sci. (U. S. A.)* **77,** 6458–6462
25. Janmey, P. A., and Matsudaira, P. T. (1988) *J. Biol. Chem.* **263,** 16738–16743
26. Yokota, E., Vidali, L., Tominaga, M., Tahara, H., Orii, H., Morizane, Y., Hepler, P. K., and Shimmen, T. (2003) *Plant Cell Physiol.* **44,** 1088–1099
27. Yokota, E., and Shimmen, T. (1995) *Plant Cell Physiol.* **36S,** s132
28. Yokota, E., Takahara, K.-i., and Shimmen, T. (1998) *Plant Physiol.* **116,** 1421–1429
29. Vidali, L., Yokota, E., Cheung, A. Y., Shimmen, T., and Hepler, P. K. (1999) *Protoplasma* **209,** 283–291
30. Yokota, E., Muto, S., and Shimmen, T. (2000) *Plant Physiol.* **123,** 645–654
31. Yokota, E., and Shimmen, T. (1999) *Planta* **209,** 264–266
32. Nakayasu, T., Yokota, E., and Shimmen, T. (1998) *Biochem. Biophys. Res. Comm.* **249,** 61–65
33. Klahre, U., Friederich, E., Kost, B., Louvard, D., and Chua, N.-H. (2000) *Plant Physiol.* **122,** 35–47
34. Schafer, D. A., Jennings, P. B., and Cooper, J. A. (1998) *Cell Motil. Cytoskeleton* **39,** 166–171
35. Karakesisoglou, I., Schleicher, M., Gibbon, B. C., and Staiger, C. J. (1996) *Cell Motil. Cytoskeleton* **34,** 36–47
36. Kovar, D. R., Staiger, C. J., Weaver, E. A., and McCurdy, D. W. (2000) *Plant J.* **24,** 625–636
37. Pollard, T. D. (1984) *J. Cell Biol.* **99,** 769–777
38. Pope, B., Gooch, J. T., and Weeds, A. G. (1997) *Biochemistry* **36,** 15848–15855
39. Schafer, D. A., Jennings, P. B., and Cooper, J. A. (1996) *J. Cell Biol.* **135,** 169–179
40. Pollard, T. D. (1986) *J. Cell Biol.* **103,** 2747–2754
41. Blanchoin, L., Pollard, T. D., and Mullins, R. D. (2000) *Curr. Biol.* **10,** 1273–1282
42. Blanchoin, L., Amann, K. J., Higgs, H. N., Marchand, J.-B., Kaiser, D. A., and Pollard, T. D. (2000) *Nature* **404,** 1007–1011
43. Bretscher, A., and Weber, K. (1980) *Cell* **20,** 839–847
44. Harris, H. E., and Gooch, J. (1981) *FEBS Lett.* **123,** 49–53
45. Maekawa, S., Nishida, E., Ohta, Y., and Sakai, H. (1984) *J. Biochem.* **95,** 377–385
46. Ashino, N., Sobue, K., Seino, Y., and Yabuuchi, H. (1987) *J. Biochem.* **101,** 609–617
47. Kurth, M. C., Wang, L.-L., Dingus, J., and Bryan, J. (1983) *J. Biol. Chem.* **258,** 10895–10903
48. Sun, H. Q., Yamamoto, M., Mejillano, M., and Yin, H. L. (1999) *J. Biol. Chem.* **274,** 33179–33182
49. Harris, H. E., and Weeds, A. G. (1984) *FEBS Lett.* **177,** 184–188
50. Bearer, E. L. (1991) *J. Cell Biol.* **115,** 1629–1638
51. McGough, A., Chiu, W., and Way, M. (1998) *Biophys. J.* **74,** 764–772
52. Yin, H. L., and Stossel, T. P. (1979) *Nature* **281,** 583–586
53. Janmey, P. A., Stossel, T. P., and Allen, P. G. (1998) *Chem. Biol.* **5,** R81-R85
54. Selve, N., and Wegner, A. (1986) *Eur. J. Biochem.* **160,** 379–387
55. Way, M., Pope, B., and Weeds, A. G. (1992) *J. Cell Biol.* **116,** 1135–1143
56. Coué, M., and Korn, E. D. (1985) *J. Biol. Chem.* **260,** 15033–15041
57. Weber, A., Pring, M., Lin, S.-L., and Bryan, J. (1991) *Biochemistry* **30,** 9327–9334
58. Janmey, P. A., Chapponier, C., Lind, S. E., Zaner, K. S., Stossel, T. P., and Yin, H. L. (1985) *Biochemistry* **24,** 3714–3723
59. Narayan, K., Chumnarnsilpa, S., Choe, H., Irobi, E., Urosev, D., Lindberg, U., Schutt, C. E., Burtnick, L. D., and Robinson, R. C. (2003) *FEBS Lett.* **552,** 82–85
60. Choe, H., Burtnick, L. D., Mejillano, M., Yin, H. L., Robinson, R. C., and Choe, S. (2002) *J. Mol. Biol.* **324,** 691–702
61. Robinson, R. C., Mejillano, M., Le, V. P., Burtnick, L. D., Yin, H. L., and Choe, S. (1999) *Science* **286,** 1939–1942
62. McLaughlin, P. J., Gooch, J. T., Mannherz, H.-G., and Weeds, A. G. (1993) *Nature* **364,** 685–692
63. Burtnick, L. D., Koepf, E. K., Grimes, J., Jones, E. Y., Stuart, D. I., McLaughlin, P. J., and Robinson, R. C. (1997) *Cell* **90,** 661–670
64. Way, M., Gooch, J., Pope, B., and Weeds, A. G. (1989) *J. Cell Biol.* **109,** 593–605
65. Kwiatkowski, D. J., Janmey, P. A., and Yin, H. L. (1989) *J. Cell Biol.* **108,** 1717–1726
66. Lin, K.-M., Mejillano, M., and Yin, H. L. (2000) *J. Biol. Chem.* **275,** 27746–27752
67. Kinosian, H. J., Newman, J., Lincoln, B., Selden, L. A., Gershman, L. C., and Estes, J. E. (1998) *Biophys. J.* **75,** 3101–3109
68. Northrop, J., Weber, A., Mooseker, M. S., Franzini-Armstrong, C., Bishop, M. F., Dubyak, G. R., Tucker, M., and Walsh, T. P. (1986) *J. Biol. Chem.* **261,** 9274–9281
69. Messerli, M., and Robinson, K. R. (1997) *J. Cell Sci.* **110,** 1269–1278
70. Pierson, E. S., Miller, D. D., Callaham, D. A., van Aken, J., Hackett, G., and Hepler, P. K. (1996) *Dev. Biol.* **174,** 160–173
71. McGough, A., Pope, B., Chiu, W., and Weeds, A. (1997) *J. Cell Biol.* **138,** 771–781
72. Gungabissoon, R. A., Jiang, C.-J., Drøbak, B. K., Maciver, S. K., and Hussey, P. J. (1998) *Plant J.* **16,** 689–696
73. Gungabissoon, R. A., Khan, S., Hussey, P. J., and Maciver, S. K. (2001) *Cell*

Motil. Cytoskeleton **49,** 104–111
74. Carlier, M.-F., Laurent, V., Santolini, J., Melki, R., Didry, D., Xia, G.-X., Hong, Y., Chua, N.-H., and Pantaloni, D. (1997) *J. Cell Biol.* **136,** 1307–1322
75. Ressad, F., Didry, D., Xia, G.-X., Hong, Y., Chua, N.-H., Pantaloni, D., and Carlier, M.-F. (1998) *J. Biol. Chem.* **273,** 20894–20902
76. Ressad, F., Didry, D., Egile, C., Pantaloni, D., and Carlier, M.-F. (1999) *J. Biol. Chem.* **274,** 20970–20976
77. Yamashiro, S., Kameyama, K., Kanzawa, N., Tamiya, T., Mabuchi, I., and Tsuchiya, T. (2001) *J. Biochem.* **130,** 243–249
78. Hussey, P. J., Allwood, E. G., and Smertenko, A. P. (2002) *Philos. Trans. R. Soc. Lond. B Biol. Sci.* **357,** 791–798
79. Miller, D. D., Callaham, D. A., Gross, D. J., and Hepler, P. K. (1992) *J. Cell Sci.* **101,** 7–12
80. Rathore, K. S., Cork, R. J., and Robinson, K. R. (1991) *Dev. Biol.* **148,** 612–619
81. Fu, Y., Wu, G., and Yang, Z. (2001) *J. Cell Biol.* **152,** 1019–1032
82. Holdaway-Clarke, T. L., and Hepler, P. K. (2003) *New Phytol.* **159,** 539–563
83. Kohno, T., and Shimmen, T. (1987) *Protoplasma* **141,** 177–179
84. Cárdenas, L., Vidali, L., Domínguez, J., Pérez, H., Sánchez, F., Hepler, P. K., and Quinto, C. (1998) *Plant Physiol.* **116,** 871–877
85. Papayannopoulos, I. A. (1995) *Mass Spectrom. Rev.* **14,** 49–71